3D MEASURES OF COMPLEXITY FOR THE ASSESSMENT OF COMPLEX TRABECULAR BONE STRUCTURES

Norbert Marwan (a), Peter Saparin (b), Wolfgang Gowin (b), Jürgen Kurths (a)
(a) Institute of Physics, University of Potsdam, Germany
(b) Charité Campus Benjamin Franklin, University Medicine Berlin, Germany

Introduction

For the assessment of bone stage (e.g. regarding different osteoporotic stages), usually the bone mineral density (BMD) is measured. However, this measurement does not contain any information about the structures inside the bone. Recent work emphasized the importance of analysing the structural changes of trabecular bone (Guo & Kim, 2002; Silva & Gibson, 1997). Different approaches for the study of trabecular bone were successfully introduced for 2D image analysis, as measures of complexity based on symbolic dynamics. The new available 3D bone images (µCT-data) challenge the development of new 3D measures of complexity, which are able to assess structural changes in trabecular bone. We consider here new developments of 3D measures based on spatial correlation and geometrical properties: Moran's *I* Index and Shape Index. Histomorphometrical measures are used for comparison with the "golden standard" of investigation of trabecular bone (Thomsen et al., 2000).

All of this is work in progress, which means that these measures may not yet be perfect and that the presented results are preliminary.

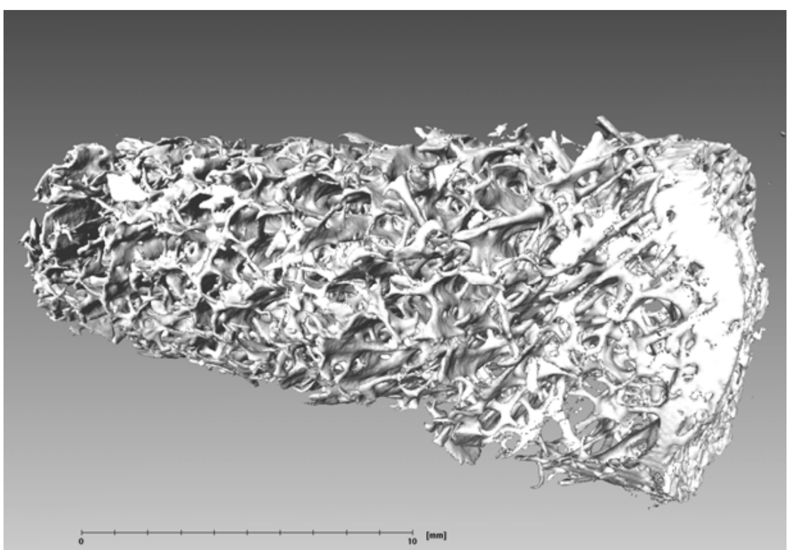

Figure 1. Complex structures in trabecular bone of proximal tibia (3D µCT scan of a biopsy).

Moran's *I* Index

Definition

The Moran test is a kind of a spatial auto-correlation test and was successfully applied in 2D image analysis (Chuang & Huang, 1992; Chen et al., 2003). The Moran's *I* Index for a two-dimensional image is defined by

$$I = \frac{N}{S_0} \frac{\sum_{j=1}^{d_1 d_2} \sum_{i=1}^{d_1 d_2} \delta_{ij} (x_i - \bar{x})(x_j - \bar{x})}{\sum_{i=1}^{d_1 d_2} (x_i - \bar{x})^2}$$

, where d_1 and d_2 are the geometric size of the image (columns and rows), x_i is the value at the specified position, $\bar{x}$ is the mean of the image, $\delta_{ij} = 1$ if pixel *i* and *j* are adjacent and 0 otherwise, $N=d_1d_2$ is the total number of pixels and $S_0 = \sum\sum\delta_{ij}$ is the number of contiguous pairs ($S_0 = 4d_1d_2 - 3(d_1 + d_2) + 2$). Its values varies between –1 and +1 (from autocorrelation $I = -1$ to negative autocorrelation $I = +1$; if not correlated, the index will be zero).

For our purpose we have to extend the 2D-definition mentioned above to a 3D-definition:

$$I = \frac{N}{S_0} \frac{\sum_{j=1}^{d_1 d_2 d_3} \sum_{i=1}^{d_1 d_2 d_3} \delta_{ij} (x_i - \bar{x})(x_j - \bar{x})}{\sum_{i=1}^{d_1 d_2 d_3} (x_i - \bar{x})^2}$$

, where S_0 is now

$$S_0 = 13d_1d_2d_3 - 9(d_1d_2 + d_2d_3 + d_3d_1) + 6(d_1 + d_2 + d_3) - 4 .$$

Pairs of contiguous neighbours must not be counted more than once. Therefore, the considered vicinity of a pixel is not a cube, but a geometric body as shown in Fig. 2.

A similar measure as the Moran's *I* Index is the Geary's *C* Index, which is an average of the variation $(x_i - x_j)^2$ between adjacent pixels. This index is inversely related to Moran's *I* Index. However, Moran's *I* Index gives a more global indicator, whereas Geary's *C* coefficient is more sensitive to differences in small neighbourhoods.

In our case of bone and marrow pixels or voxels, these measures are related to an investigation of the interface between bone and marrow.

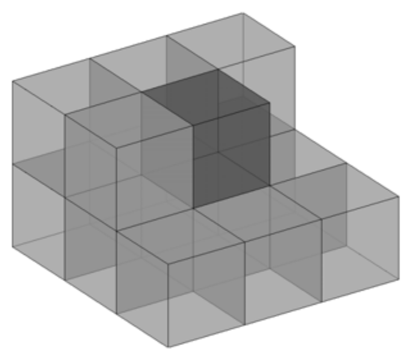

Figure 2. Contiguous neighbours (gray) of a voxel (darkgray) in 3D.

Moran's *I* Index of Proximal Tibia

Now we apply the Moran's Index to real µCT bone data gained from proximal tibia biopsies (1cm VOI used). First, we plot the Moran's Index in respect of BV/TV (Fig. 3). Next, we plot this index over to the so-called node-terminus ratio, which is a histomorphometrical measure expressing the connectivity of the trabecular network. Whereas both figures reveal a dependence between these measures, the Moran's *I* Index correlates more significantly with the node-terminus ratio (lin. correlation is 0.65; with BV/TV is 0.54). The result of the Geary's *C* Index is similar (here not shown).

From these results we infer, that the measures based on spatial correlations are closely related with the connectivity of the trabecular network.

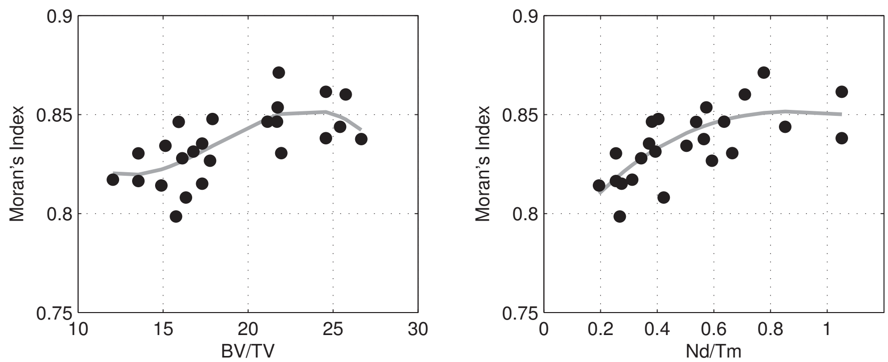

Figure 3. Morans's *I* Index over BV/TV and node-terminus ratio Nd/Tm.

Shape Index

Definition

For an object with a given volume, the surface depends on its geometric shape: its surface is minimal for the shape of a sphere

$$S_{sphere} = \sqrt[3]{36\pi V^2} = \text{minimal.}$$

Therefore, the ratio between the bone surface S_{bone} and the minimal surface S_{sphere}, is introduced:

$$SHI = \frac{S_{bone}}{S_{sphere}}.$$

Such a measure should be able to distinguish between shapes like plates and rods or angular and rounded objects.

This ratio can be computed within gliding boxes in order to get a distribution of this index, which can be further quantified, for instance by using average or entropy.

A brief note about the estimation of the surface and the volume of a discrete three-dimensional object: Our data consist of voxels of zero and one (one means bone and zero means marrow). The simplest approach would be to count the bone voxels for the volume and sum their surfaces. However, these are rather bad estimators for surface and volume – especially when we use an equation in order to compute the minimal surface. Therefore we use an iso-surface algorithm in order to estimate the bone surface and volume. Whereas the code for the iso-surface algorithm for surfaces is widely distributed, for instance for 3D visualization, the code for the volume estimation has not yet been available and was implemented in our group.

Shape Index of Proximal Tibia

First we are interested in the joint-distributions of the Shape Index and the found volume within small sliding boxes (box size 400μm) regarding different osteoporotic stages (Fig. 4).

Due to the bone mass the main point of the distribution slips to higher bone volumes for higher BV/TV. But in the same time this main point moves towards smaller Shape Index values. For higher BV/TV or healthy bone, the distributions are more horizontal, whereas for osteoporotic bone the distributions are more vertical oriented. For the intermediate stage, the distributions seems to be smeared.

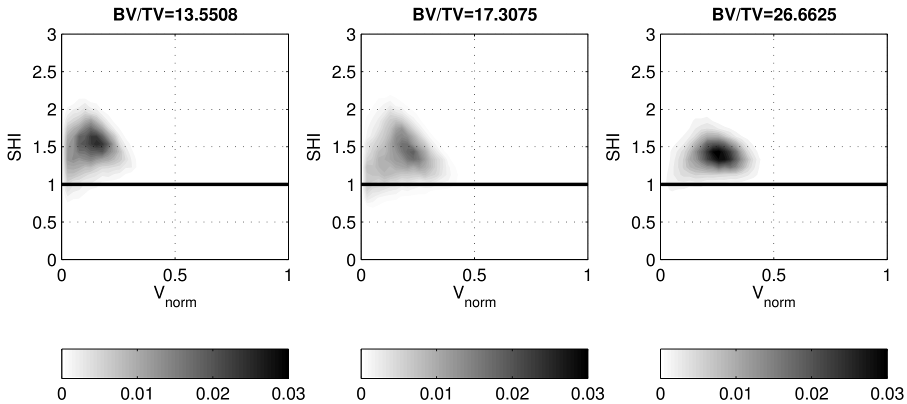

Figure 4. Joint distributions of shape index and bone volume for various osteoporotic stages.

Whereas these remarks are only visual inspections of the distributions, these changes can be quantified with statistical measures (Figs. 5, 6).

The mean of the shape index and the entropy of its distribution increase for decreasing BV/TV. However, the mean shape index correlates better with a histomorphometrical measure, the node-terminus ratio, suggesting a correlation between the mean Shape Index and the connectivity. The entropy correlates well with another histomorphometrical measure – the trabecular plate separation. This parameter reveals the relationship between the shape of the distribution and the amount of parallel structures in the trabecular network.

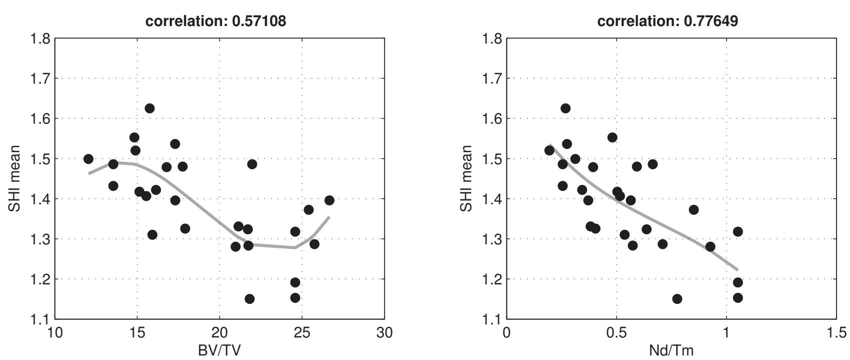

Figure 5. Mean shape as function of BV/TV and node-terminus ratio Nd/Tm.

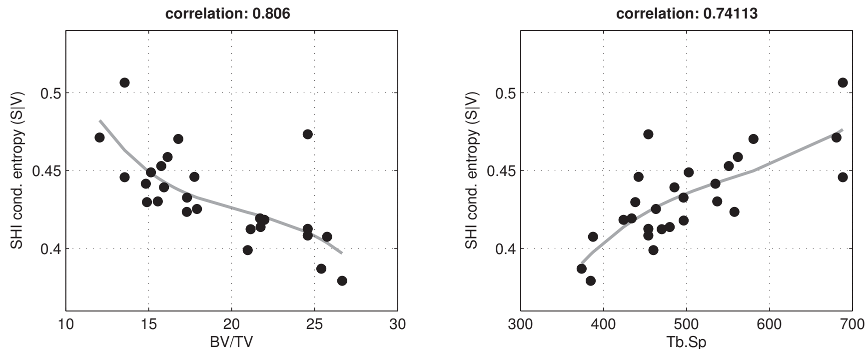

Figure 6. Entropy of shape index as function of BV/TV and trabecular plate separation Tb.Sp.

Conclusions

In the presented work the well-known 2D measures of complexity Moran's *I* and Geary's *C* Index were successfully adopted to 3D. The Moran's *I* and Geary's *C* Index are related with the network connectivity.

Then a new 3D measure was introduced, which is called Shape Index and which uses simple geometrical features. The Shape Index is related with several histomorphometrical measures (connectivity, parallel plate model, star volume). At the moment this measure is our most promising candidate for the investigation of complex structures in trabecular bone.

Using the proposed measures we found significant changes in 3D bone architecture (connectivity, plate separation) at various stages of osteoporosis.

Acknowledgements

This work is supported by the ESA-Project AO-99-030 *Bone 3D* (contract #14592).

References

Chen, T.-J., Chuang, K.-S., Wu, J., Chen, S. C., Hwang, I.-M., Jan, M.-L., A novel image quality index using Moran *I* statistics. Journal of Digital Imaging 16 (2), 2003, 210-215

Chuang, K.-S., Huang, H. K., Assessment of noise in a digital image using the joint-count statistic and the Moran test. Physics in Medicine and Biology 37 (2), 1992, 357-369

Guo, X. E., Kim, C. H., Mechanical Consequence of Trabecular Bone Loss and Its Treatment: A Three-dimensional Model Simulation. Bone 30 (2), 2000, 404-411

Silva, M. J., Gibson, L. J., Modeling the Mechanical Behavior of Vertebral Trabecular Bone: Effects of Age-Related Changes in Microstructure. Bone 21 (2), 1997, 191-199

Thomsen, J. S., Ebbesen, E. N., Mosekilde, Li., A New Method of Comprehensive Static Histomorphometry Applied on Human Lumbar Vertebral Cancellous Bone. Bone 27 (1), 2000, 129-138